STATISTICAL METHODS FOR THE HF PRIMARY POWER STANDARD REALIZATION

L. Brunetti, L. Oberto, M. Sellone

Istituto Nazionale di Ricerca Metrologica (INRIM), strada delle Cacce 91, 10135, Torino, Italy, l.brunetti@inrim.it

Abstract: A coaxial microcalorimeter based on thermoelectric detection is the system used to realize the broadband primary power standard at high frequency by Istituto Nazionale di Ricerca Metrologica, Italy. The paper describes and compares two analysis methods that can be applied to the measurement data for evaluating the overall system uncertainty. Methods are completely general and we applied them to our measurement system that can operate with 7 mm, 3.5 mm and 2.92 mm coaxial insets, covering, therefore, the frequency range of 10 MHz - 40 GHz.

Key words: Measurement standards, microwave measurements, power measurements, thermoelectric devices, transmission line measurements.

1. INTRODUCTION

Coaxial and waveguide microcalorimeters based on the bolometric detection are the systems used by primary laboratories for implementing the high frequency (HF) power standards, [1-6]. Conversely, the Istituto Nazionale di Ricerca Metrologica (INRIM), Italy, developed a coaxial microcalorimeter that uses a thermoelectric power sensor as thermal load [7]. This solution was initially adopted for working around the difficulty to find commercial coaxial bolometers for frequencies beyond 26.5 GHz. In the meanwhile, thermoelectric sensors turned out to be an excellent alternative to classic bolometers, so that INRIM decided to implement its power standards by using such technical solution only [8]. Two coaxial microcalorimeters now exist in the INRIM HF-laboratory, which can be fitted with 7 mm, 3.5 mm and 2.92 mm feeding lines. Depending on the line configuration selected, we can, therefore, determine the effective efficiency of dedicated thermoelectric power sensors up to 40 GHz.

To our knowledge, a lack in the literature exists concerning data analysis models in microcalorimetric measurements. No papers have been recently published on the subject. Very scarce also are microcalorimeter theories that propose alternative approaches to the measured correction for obtaining an estimation of the effective efficiency without systematic errors, in recent times at least [2], [9], [10]. Conversely, the need of reducing the measurement uncertainty leads to refining data analysis procedures and mathematical models.

In this paper, two different methods for data analysis are detailed. We call them the Multiple Value Method (MVM) and the Single Value Method (SVM). We also present a comparison between the outcomes of the two procedures when applied to measurements at some significant frequencies used in international key comparisons.

Some considerations have been done on which of the two methods takes better into account the major contribution to the measurement uncertainty (that is the thermal drift as we will see in Section 4.2). In doing this, we describe additional non-routine measurements performed both to validate our microcalorimeter model and to establish a statistics for the experimental data. This step is very important in order to perform a correct assessment of the system uncertainty.

In Section 2 the INRIM microcalorimeter is briefly described. Some notes on its mathematical model are also given. Section 3 presents a description of the measurement procedure and of the data recorded by the automatic instrumentation system. The methods MVM and SVM for data analysis are, instead, introduced in Section 4 and compared in Section 5. Finally conclusions are drawn in Section 6.

2. THE MEASUREMENT SYSTEM AND ITS MATHEMATICAL MODEL

The structure of a coaxial thermoelectric microcalorimeter used by INRIM has been widely described in the literature by the same authors [7], [8]. Briefly, it is an adiabatic system whose kernel consists of two twin coaxial lines that supply electromagnetic power to dedicated power sensors trough a complex of thermal shields as Fig. 1 shows.

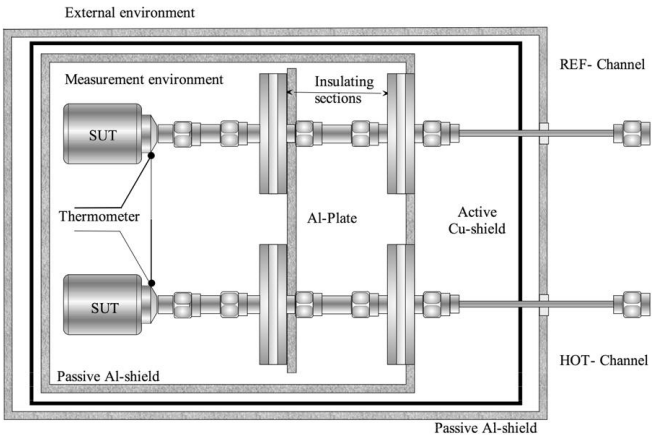

Fig. 1. Scheme of an INRIM coaxial microcalorimeter kernel. The key elements for a proper thermal stabilization, that are the feeding lines, the insulating sections, and the active and passive shields of the thermostat, are depicted.

This technical solution is necessary in order to insulate the sensor under test (SUT) from the external environment and to provide a measurement chamber with a thermal stability of few mK. Indeed, the electrical thermometer, which measures the temperature at the power sensor input, must be able to sense power losses whose effects may be in the mK range and, possibly, even below.

The measurement system is fully under PC control via IEEE 488.2 GPIB bus. Dedicated software allows the complete automation of the measurement procedure and data taking.

The relation between the measurand, that is, the power sensor effective efficiency η_e and the thermometer asymptotic voltage response e has been demonstrated to be [8]:

$$\eta_e = \frac{e_2}{e_1 - e_{1SC}}, \quad (1)$$

where e_1 is the asymptotic temperature reached by the SUT input when supplied with HF power, e_2 the temperature obtained after an appropriate substitution with a low frequency (LF) power, while e_{1SC} is the response when half of the HF power generating e_1 is supplied to a totally reflective load. The term e_{1SC} is a correction related to feeding line losses. Model (1) can be refined including other terms related to short circuit losses, imperfect power substitution [9], [10] and to the SUT reflection coefficient. However, these correction terms turned out to be only minimal in the uncertainty budget. Therefore, for simplicity, in this work they are neglected.

3. MEASUREMENT PROCEDURE AND MICROCALORIMETER DATA

Microcalorimetric measurements consist of two steps: SUT and system calibration. In the SUT calibration step, the twin feeding lines are terminated with twin sensors, one as SUT and the other as thermal reference. During the calibration step, instead, the feeding lines are terminated with reflecting loads specifically designed to be thermally equivalent to the SUT. Independently of the step, the thermometer response waveform has the typical behavior shown in Fig. 2.

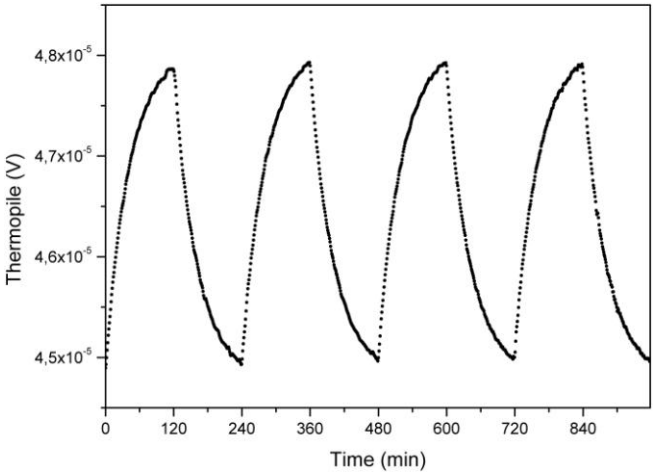

Fig. 2. Thermometer response when power is supplied to a matched SUT switching between HF power and reference power.

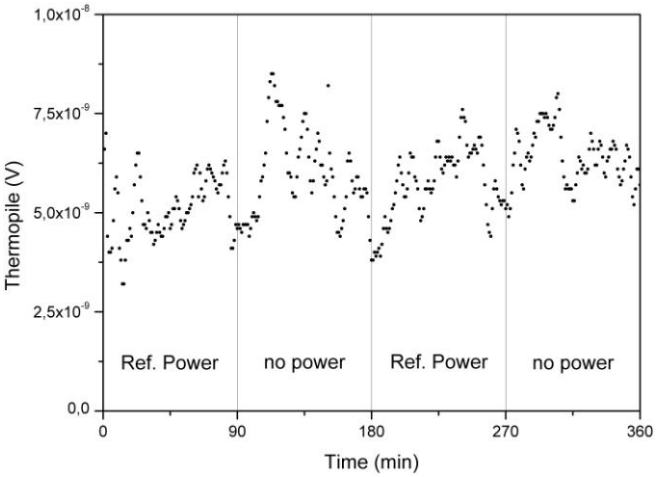

Fig. 3. Thermometer response when the reference power is switched on and off and the microcalorimeter feeding line is short circuited.

The increasing fronts are relevant to the heating produced by HF-power injection into the SUT or into the reflecting load while the decreasing fronts are related to the cooling consequent to loss reduction after power substitution at 1 kHz, which is the reference frequency adopted. The switching time is around 3 time constants to ensure fitting results with the highest precision possible and minimum time consuming. A similar but lower signal is obtained in the microcalorimeter calibration step during which the feeding lines are terminated with the reflecting loads.

Only the asymptotic voltages corresponding to the temperatures reached by the thermal load, i.e., SUT plus connection components or the reflecting load plus connection components, enter in (1). For the INRIM systems, figures are of the order of 40 μV during the SUT calibration step and 1 μV during the system calibration step with the reflecting load.

4. DATA ANALYSIS

Before the data analysis it is necessary to check the validity of the adopted model. Equation (1) is valid only if the hypothesis of null line losses at the 1 kHz reference power holds [9]. To verify this condition we performed a series of measurements, by switching on – off the reference power when the microcalorimeter feeding line is short–circuited. If the hypothesis holds, the thermopile voltage must not change and, in facts, this is the case as can be seen in Fig. 3 where a short selection of the recorded data is shown. Then, three ways are feasible for obtaining the mentioned thermal asymptotes:

I. To perform several heating – cooling steps and to fit independently each increasing or decreasing curve with exponential functions. Then mean asymptote values are computed;
II. To consider a single power substitution cycle with a large switching time (larger than 10 time constants). In this case asymptote values are directly measured by thermopile at the end of each semi-cycle;
III. To execute a single power substitution cycle with a large (or medium) switching time and to fit this single curve to obtain the desired asymptotes.

The three ways should produce the same result, unless anomalous conditions occur. Anyway solution I is considered more reliable because it allows taking into account the influence of external factors on the measurement repeatability and to better observe the presence of a drift due, for example, to thermal instability, if any. Once the *e*-asymptotes are found by adopting the first solution and the effective efficiency is calculated with (1), the uncertainty has to be evaluated.

Two different methods are used which are described in the following.

4.1. Multiple Value Method

With Multiple Value Method (MVM) we mean the consideration of a single heating and cooling cycle. Measurements are performed both with the feeding line terminated with the SUT and with the reflecting load. The values of the three asymptotes needed by (1) are found by a fitting process that requires type A and B uncertainty of every measurement point, thus obtaining a value η_{e1} of the effective efficiency with an uncertainty comprehensive of both type of contributions. Type A uncertainty is given by the measurement dispersion whereas type B is evaluated from the instrument specifications. The system has been optimized in order to eliminate other possible sources of systematic contribution such as substitution errors [10] and feeding lines imbalance [12].

This procedure is repeated for every power substitution, collecting, in this way, many effective efficiency values η_{ei} ($i \in [1, \dots, N]$, N = number of power substitution) that are, then, averaged:

$$\eta_e = \frac{1}{N}\sum_{i=1}^{N}\eta_{ei}. \tag{2}$$

Total measurement uncertainty is given by the standard deviation of the mean of the effective efficiency values. If η_{ei} have not nearly the same uncertainty, a weighted mean is a better solution. The expanded uncertainty $U(\eta_e)$ is obtained multiplying $u(\eta_e)$ by the proper coverage factor k (normally equal to 2).

Usually no other measurements are performed. This method relies heavily on the hypothesis that the effective efficiency values are sampled from a Gaussian distribution. It has been widely used in past years, especially at INRIM often in conjunction with very long switching time (solution II mentioned in the previous section).

4.2. Single Value Method

We refer to Single Value Method (SVM) when considering the whole set of measurement cycles at the same time.

In this way, a set of asymptotes e_{1i} ($i \in [1, \dots, N]$, N = number of cycles) is found from the heating phases, a set of e_{2i} is collected considering the cooling phases; e_{1SCi} is found calculating the asymptotes of the heating period of the waveform obtained during the microcalorimeter calibration cycles performed with the reflecting load.

Each data set is averaged to find a single value for each asymptote e_1, e_2 and e_{1SC}:

$$e_k = \frac{1}{N}\sum_{i=1}^{N} e_{ki}, \tag{3}$$

in which k = 1, 2, 1SC. These averages make sense if the elements of each set to be averaged have the same uncertainty. This condition is easily met in practice, otherwise, again a weighted mean should be a better solution:

$$e_k = \frac{\sum_{i=1}^{N}\frac{e_{ki}}{\sigma(e_{ki})^2}}{\sum_{i=1}^{N}\frac{1}{\sigma(e_{ki})^2}}, \tag{4}$$

in which $\sigma(e_{ki})$ is the uncertainty of the fitting procedure.

It is important to note that the values obtained with (3) or (4) are affected by systematic errors.

In fact, if the two feeding lines and sensors are perfectly twin, the thermopile output voltage must be null when no signals are supplied to the system (neglecting the contribution of the instrumentation noise). The thermopile reads the temperature difference between the inputs of the two sensors terminating the feeding lines, indeed. In practice, a null voltage is impossible to attain because of several possible sources of systematic bias such as thermovoltages, bias current of the nanovolt amplifier used to measure the thermopile voltage and less–than–perfect balance of the feeding lines. The system has been designed to reduce to a minimum, possibly negligible extent, these contributions, however the measurement of the thermopile voltage, once the system is thermally stabilized and not supplied with any signal, is a measure of the thermal imbalance of the twin–line complex. We measured figures of about 6 nV. Moreover we measured a bias current of the nanovolt amplifier of 20 pA. Considering that the thermopile system has a resistance of about 300 Ω, it is straightforward that the measured bias voltage is due to the bias current of that amplifier. That means that all other sources of systematic bias are correctly removed and that the system is thermally balanced. To eliminate also this bias, the voltage should be subtracted from the every thermopile voltage measurement. In our case, since the microcalorimeter has a good thermal symmetry between the feeding lines, this contribution is very small and, often, negligible but, generally speaking, it should be taken into account. Its uncertainty $u(v_a)$ has also to be included in the uncertainty budget as type B contribution. Anyway it turned out to be the smallest contribution.

Now, to evaluate the uncertainty of the effective efficiency obtained as described above, the law of the propagation of the uncertainties [11] has to be applied and, therefore, we need to know the uncertainty of the asymptotic values calculated with (3) or (4). To our opinion, for a proper asymptote uncertainty assessment, supplementary measurements are necessary, so to establish the system noise floor, the repeatability of the asymptotes evaluation and, eventually, to reduce possible drifts in the thermopile output [12]. The random noise contribution to the asymptote values can be found simply evaluating the standard deviation of the

mean $u(e_k)_{std}$ of each data set or, if (4) is used, with the following relation:

$$u(e_k)_{std} = \frac{1}{\sqrt{\sum_{i=1}^{N} \frac{1}{\sigma(e_{ki})^2}}}. \quad (5)$$

Nevertheless, in ordinary laboratory practice, the execution of many cycles is impossible because the system time constant is of the order of 40 minutes. If measurements last 3 time constants to ensure a good fitting outcome, a single cycle requires 4 hours for a single frequency point. As a consequence, to perform tens of cycles for a good statistics and covering, at the same time, a wide frequency band is cumbersome. Therefore repeated measurements of many cycles can be done only once, as a supplementary measurement, for evaluating the repeatability contribution to be taken into account during the uncertainty analysis. The repeatability obtained in this way can be used in data analysis as a typical figure. In ordinary practice, only few measurement cycles have to be done in order to check the stability is maintained in time. For example, 50 measurement cycles of the SUT at the frequency of 18 GHz give the following results:

$$\begin{cases} e_1 = (4.56090 \pm 0.00078) \cdot 10^{-5} \text{ V} \\ e_2 = (4.16715 \pm 0.00056) \cdot 10^{-5} \text{ V} \end{cases}. \quad (6)$$

Furthermore, a hidden contribution has not been accounted for. Indeed, even if the short-term temperature stability of the microcalorimeter inner chamber is be very good, long-term measurements could be affected by a residual temperature drift that results in an analogous drift of the asymptotic values (directly or inversely correlated). This effect is due, mainly, to small room temperature variations that still bypass the insulating sections of the feeding lines. Moreover, bigger variations could be present that affect the measurement chamber of the thermostat through the walls without being sufficiently smoothed by the stabilization system.

For example, a rise of the asymptotic value is observed corresponding to a decrease of the thermostat temperature as it can be seen in Fig. 4. Indeed, if the thermostat temperature increases, also the temperature of the cold pole of the thermopile rises causing a decrease of the thermopile output voltage. Moreover, in the same picture it is shown that an abrupt increase of the temperature causes a strong instability in the asymptote and that the two quantities are inversely proportional.

Anyway, the asymptote uncertainty is calculated as root sum of squares of all the contributions evidenced in this section:

$$u(e_k) = \sqrt{u(e_k)_{std}^2 + u(e_k)_{drift}^2 + u(v_a)^2} \quad (7)$$

in which k = 1, 2, 1SC and v_a is the thermopile contribution due to the system imbalance.

Fig. 5 presents a record of e_1 from which the slope is calculated by means of a linear fit. Measurements lasted for 50 cycles of 4 hours each. In this case the drift is about 0.01

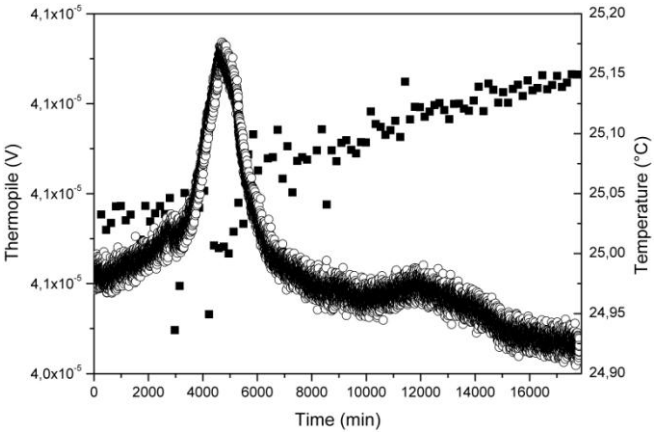

Fig. 4. Effect of temperature variations on the asymptote e_1. Squares are the asymptotic values of the thermopile readings while circles are measurements of the inner shield temperature of the microcalorimeter thermostat.

nV/min but the typical trend of the experimental results is about 1 nV/min. If one performs only 4 measurement cycles, the contribution of the drift cannot be easily seen in the data.

This could induce the operator to neglect an uncertainty contribution that cannot be neglected because, for 4 measurement cycles, its contribution can reach 80 nV.

The drift is not always present in the same way, therefore, to our opinion, a sufficiently conservative decision is to evaluate the maximum thermal drift contribution and to consider this value as typical.

Following this criterion and assigning a rectangular distribution to the drift, the results in (6) become:

$$\begin{cases} e_1 = (4.5609 \pm 0.0082) \cdot 10^{-5} \text{ V} \\ e_2 = (4.167 \pm 0.012) \cdot 10^{-5} \text{ V} \end{cases}. \quad (8)$$

A slightly higher contribution is observed for e_2. Drift correction applies to the reflecting load measurements also.

An example of uncertainty budget for e_1 is given in table 1. The most important contribution arises from the thermal drift that, therefore, must be well controlled. Very important is the repeatability also of the asymptote determination that is only slightly lower. Conversely the contribution due to the correction of the nanovolt amplifier bias current is

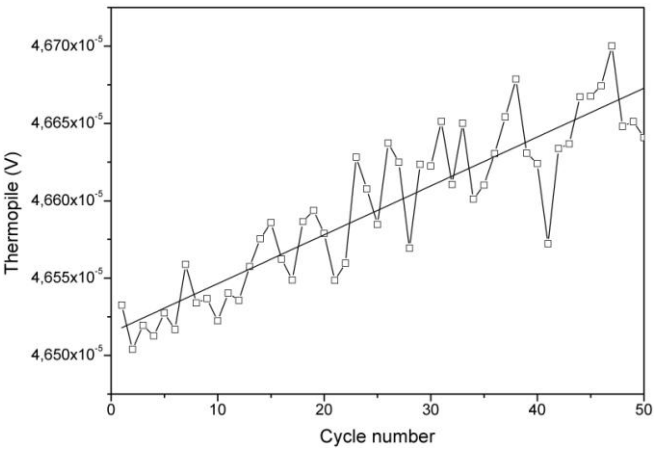

Fig. 5. Example of e_1 thermal drift at 18 GHz during 50 4-hour measurement cycles. Squares are measured values and thin lines are a guide for the eye. The thick line is the linear fit of the data.

Table 1. Uncertainty budget for an evaluation of the asymptote e_1.

Contribution	Value / V
$u(e_k)_{std}$	$7.84 \cdot 10^{-9}$
$u(e_1)_{drift}$	$8.03 \cdot 10^{-8}$
$u(v_a)$	$1.47 \cdot 10^{-11}$
$u(e_1)$	$\mathbf{8.21 \cdot 10^{-8}}$

negligible. Similar results are obtained for e_2 and e_{1SC}.

The uncertainty of η_e is found applying the law of the propagation of uncertainties to (1) according to [11]:

$$u(\eta_e) = \sqrt{\frac{e_2^2\left[u(e_1)^2 + u(e_{1SC})^2\right] + \left[u(e_2)(e_1 - e_{1SC})\right]^2}{(e_1 - e_{1SC})^4}} . \quad (9)$$

In a thorough analysis, the terms e_1, e_2 and e_{1SC} are correlated through the thermal drift and, therefore, a correlation term should appear in (9). Anyway we verified that, in our case, this term is negligible being about three orders of magnitude below the contributions due to e_1 and e_2 and one order of magnitude below the contribution related to e_{1SC}. The expanded uncertainty $U(\eta_e)$ is, then, evaluated multiplying $u(\eta_e)$ by the proper coverage factor k (usually equal to 2).

5. METHODS COMPARISON

A comparison between the MVM and SVM procedures is presented in Table 2. It lists figures evaluated from the data analysis of 4 measurement cycles of a thermoelectric power sensor [8] at some typical CCEM key comparison frequencies.

As it can be seen, the outcomes of the two different methods differ significantly. In particular, while the effective efficiency value is the same, the MVM procedure gives uncertainties that are about one order of magnitude lower. Of course, this difference reduces if the thermal drift is eliminated.

In any case, since these measurements are very time consuming, the operator cannot always repeat the measurements even if, during the data analysis, he notices that a drift has occurred. In this case, the SVM takes into account better this contribution.

Furthermore, to our opinion the SVM is more appropriate not only because it accounts for the temperature drift, that is the major contributor to the asymptotes uncertainty, but also because it results in a smaller bias as demonstrated in [13-15]. In this situation the lower uncertainty produced by the MVM can be the result of an underestimation. Moreover, the MVM supposes that the distribution of the η_{ei} is Gaussian in attributing the standard deviation of the η_{ei} -set as the uncertainty of the mean effective efficiency.

This assumption has to be verified every time with a large number of measurement cycles.

To our opinion, it does not hold in general due to the effect of the temperature drift that causes a linear increase or decrease of the asymptotes (see Fig. 6).

It is also possible that the trend is different between the SUT calibration phase
and the system calibration phase.

Conversely, the SVM does not rely on the Gaussian hypothesis and, therefore, allows a proper treating of different drifts during different measurement stages.

Table 2. Comparison between MVM and SVM analysis procedures at some typical Key Comparison frequencies. Expanded uncertainty $U(\eta_e)$ is evaluated using coverage factor k=2.

Frequency	Method	η_e	$U(\eta_e)$
50 MHz	MVM	0.9921	0.0004
	SVM	0.9921	0.0064
18 GHz	MVM	0.9502	0.0009
	SVM	0.9502	0.0065
26.5 GHz	MVM	0.8746	0.0021
	SVM	0.8746	0.0098

6. CONCLUSION

This paper reports the comparison between two different data analysis in the evaluation of the effective efficiency of thermoelectric power sensors by using the microcalorimetric technique.

Non-routine operations are also presented, aimed to suppress systematic contributions, to identify and take into account measurement biases and drifts. The need of these measurements is highlighted in the framework of the SVM that we consider most suitable also from the statistical point of view.

A comparison between the two procedures shows the significant difference between the uncertainties produced by the two approaches in presence of a significant thermal drift.

As an example, measurements performed at typical frequencies at which international comparisons have been carried out are reported. It is seen that the MVM produces underestimated uncertainties, about 10 times lower than those produced by the SVM.

ACKNOWLEDGMENT

The authors would like to thank their colleague Paolo Terzi for the help in preparing the microcalorimeter set-up and Dr. Adriana Manenti for paper revision.

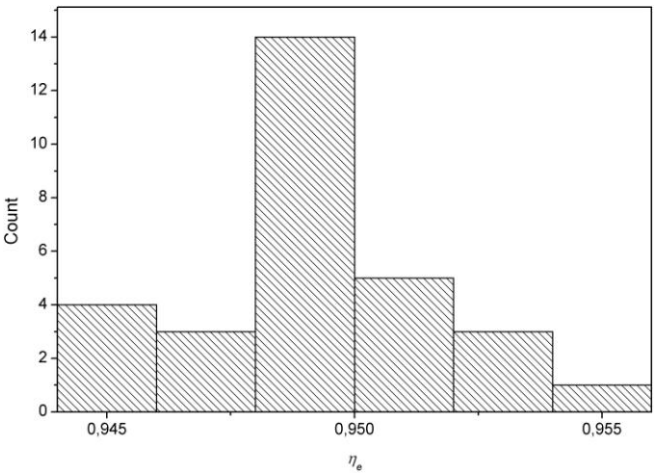

Fig. 6. Example of non–Gaussian distribution of the effective efficiency due to thermal drift.

REFERENCES

[1] A. Fantom, Radiofrequency and microwave power measurement. London, U.K.: Peter Peregrinus Ltd., 1990.

[2] R. Judaschke and J. Ruhaak, "Determination of the correction factor of waveguide microcalorimeters in the millimeter-wave range", IEEE Trans., vol. IM-58, no. 4, pp. 1104–1108, Apr. 2009.

[3] Y. Okano and T. Inoue, "Automatic microcalorimeter system for broadband power measurement in 75-110 GHz range", IEEE Trans., vol. IM-50, no. 2, pp. 385–388, Apr. 2001.

[4] R. Clark, "The microcalorimeter as a national microwave power standard", Proc. IEEE, vol. 74, no. 1, pp. 102–104, Jan. 1986.

[5] D. L. Hollway and W. Muller, "The precise measurement of the RF power and voltage using coaxial calorimeters and microcalorimeters", IEEE Trans., vol. IM-33, no. 4, pp. 269–275, Dec. 1984.

[6] S. A. Kolotygin, L. T. Konkova and V. G. Chuiko, "Measurement of the effective efficiency of a coaxial thermal transducer in a microcalorimeter at 18 GHz", Meas. Tech., vol. 22, no. 10, pp. 1253–1256, Oct. 1979.

[7] L. Brunetti and E. Vremera, "A new microcalorimeter for measurements in 3.5-mm coaxial line", IEEE Trans., vol. IM-52, no. 2, pp. 320–323, Apr. 2003.

[8] L. Brunetti, L. Oberto and E. Vremera, "Thermoelectric sensors as microcalorimeter load", IEEE Trans., vol. IM-56, no. 6, pp. 2220–2224, Dec. 2007.

[9] L. Brunetti and L. Oberto, "On coaxial microcalorimeter calibration", Eur. Phys. J. App. Phys., vol. 43, pp. 239–244, Aug. 2008.

[10] L. Brunetti, L. Oberto, M. Sellone and E. Vremera, "Comparison among coaxial microcalorimeter models", IEEE Trans., vol. IM-58, no. 4, pp. 1141–1145, Apr. 2009.

[11] JCGM (2008). Evaluation of measurement data – Guide to the Expression of Uncertainty in Measurement (GUM 1995 with minor corrections) JCGM 100:2008 [Online]. http://www.bipm.org/utils/common/documents/jcgm/JCGM_100_2008_E.pdf.

[12] L. Brunetti, L. Oberto, M. Sellone and E. Vremera, "Analysis methods of coaxial microcalorimeter data", in Proc. 27th Conference on Precision Electromagnetic Measurements, Daejeon, Korea, 2010, p. 706–707.

[13] W. Bich, L. Callegaro and F. Pennecchi, "Non-linear models and best estimates in the GUM", Metrologia, vol. 43, pp. S196–S199, 2006.

[14] L. Oberto and F. Pennecchi, "Estimation of the modulus of a complex–valued quantity", Metrologia, vol. 43, pp. 531–538, 2006.

[15] F. Pennecchi and L. Oberto, "Uncertainty evaluation for the estimate of a complex–valued quantity modulus", Metrologia, vol. 47, pp. 157–166, 2010.